UDC 621.316.54

Development and Application of Mechanical Switches

By Masami Ishizawa, Hideo Nabetani and Ryohei Kinoshita

(Manuscript received March 24, 1980)

Because keyboards are the point of contact between man and machine, their performance must respond to both operators' and system designers' demands.

These demands are summarized in three points:

1) Good operational characteristics

2) High reliability

3) Low cost.

This paper describes the design and characteristics of a mechanical switch which can be applied to two types of keyboard, sheet-type keyboard and typewriter keyboard, and shows excellent performance in regard to all three of the points above.

1. Introduction

Keyboards are now extensively used in many kinds of computer terminals, electronic cash registers, and microcomputer-equipment, and recently their applications have been expanding and diversifying into the areas of measuring instrument consoles, numerical control machines, and even game machines.

At the same time, keyboard performance demands by both operators and system designers are growing more and more stringent. The keyboard is, after all, the point of contact between man and machine. Moreover, the proliferation of

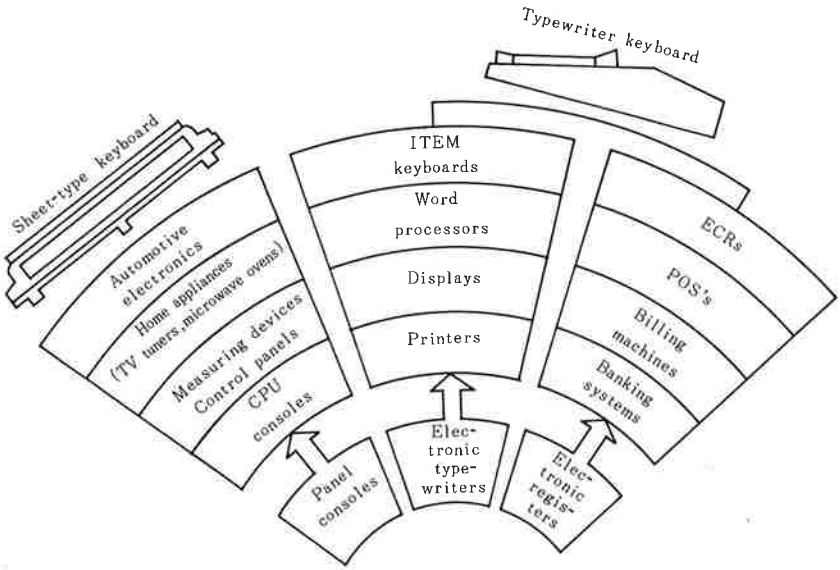

Fig. 1—Variations of keyboard.

electronic equipment in the general market has raised the need for cost reduction.

As shown in Fig. 1, keyboards can be grouped according to their construction into two types; sheet-type keyboards and typewriter keyboards. This paper describes a new mechanical switch which can be applied to either type of keyboard and combines excellent operational characteristics, high reliability, and economy.

Using this switch, a sheet-type keyboard whose surface is covered with a plastic sheet and a typewriter keyboard with individual keytops have been developed.

The principal features of the new switch and keyboards are as follows:

2. Operational characteristics

The experimental data shown in Fig. 2 were used to determine optimum

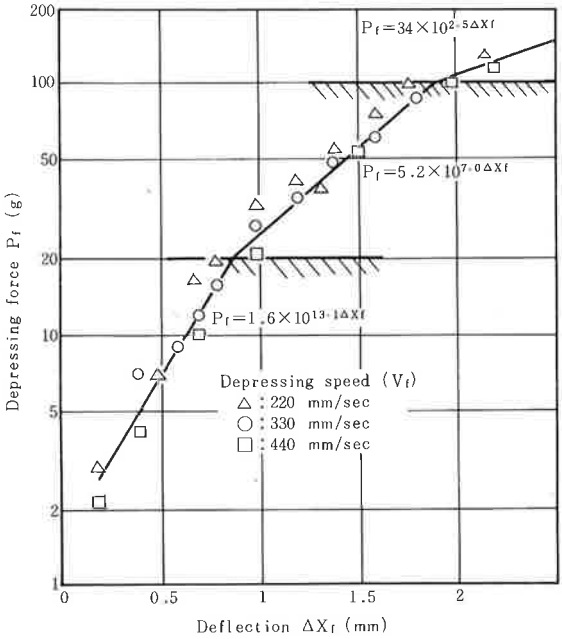

Fig. 2—Dynamic characteristics of the human finger.

operational characteristics[1]. It was found that the dynamical elastic characteristics of the operator's finger approximated a straight line. This is due to the elasticity of the fingertip and motion of the knuckle. If the depressing force of the keyboard corresponds to the values within the hatched portion of Fig. 2 (20 to 100 g), the operator can operate the keyboard continuously and comfortably without fatigue. Furthermore, a snap-action switch which provides tactile and audible feedback to operator is useful to help him or her avoid mistakes.

The optimum operational characteristics were defined as shown in Fig. 3.

The construction of spring shown in Fig. 4 was designed to realize these optimum operational characteristics in an economical way. Figure 4 shows a cross section of this switch. The dome-spring is a spherical metalic plate and the actuator is a plate-spring which forms a contilever. The triangles under the dome-spring show contacts.

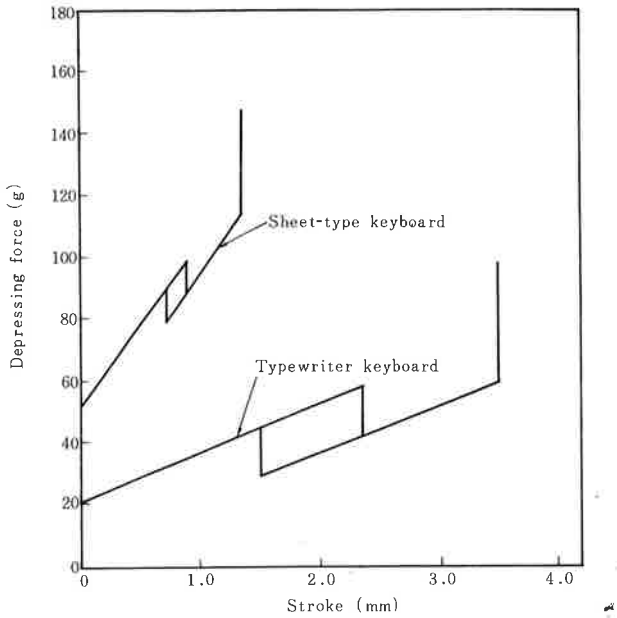

Fig. 3—Operational characteristics.

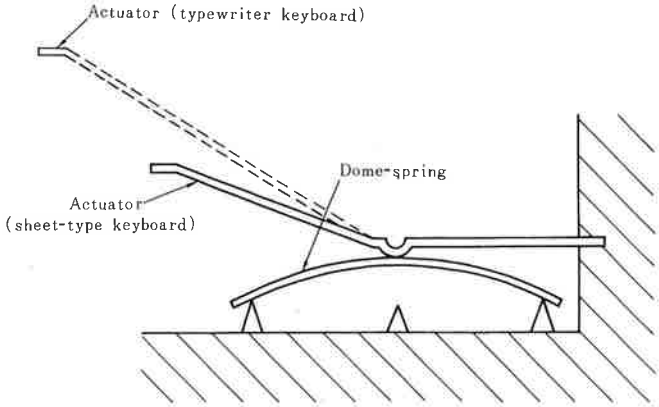

Fig. 4—Construction of spring.

When the actuator is pushed down, the dome-spring set on the outer contacts deforms, then snap through and finally touches the inner contacts, so that both contacts are electrically connected. With this construction the repulsive force of the dome-spring provides the snap action of a mechanical switch, while the actuator reduces the repulsive force and permits stroke length to vary freely.

2.1 Design of dome-spring

On account of complicated shape, the finite element method was used to analyze spring characteristics. It is clear that the dome-spring can be considered as a shell, but a large number of elements might be required if general plate-element analysis was applied. So the authors simplified the analysis by taking the dome-spring as an axi-symmetric shell.

Next, the dome-spring shows a buckling characteristic called "snap-through" or "oil canning" in the deforming process. This is a typical example of a large scale deformation problem and can be understood as a classical "elastica" problem. In this way, the dome-spring shows non-linear spring characteristics. It is possible to lead this to an analysis based on the theory of small scale deforming by adapting incremental theory. This is to repeat the next process step by step.

For an elastic problem, the relation of force and displacement is shown by equation (1).

$$\{P\} = [K]\{d\} , \qquad \cdots\cdots\cdots\cdots\cdots\cdots\cdots\cdots (1)$$

where,

$\{P\}$: Nodal force vector

$[K]$: Stiffness matrix of structure

$\{d\}$: Nodal displacement vector.

Generally, an analysis by the finite element method begins with obtaining the element stiffness matrix. In the case of this dome-spring, each element was established for an axi-symmetric conical frustum element. The element stiffness matrix was given by Zienkiewicz[2]. Following his method, the stiffness matrix of an element was obtained as follows (see Fig. 5).

$$[K] = \int [B]^T[D][B]dv , \qquad \cdots\cdots\cdots\cdots\cdots\cdots\cdots\cdots (2)$$

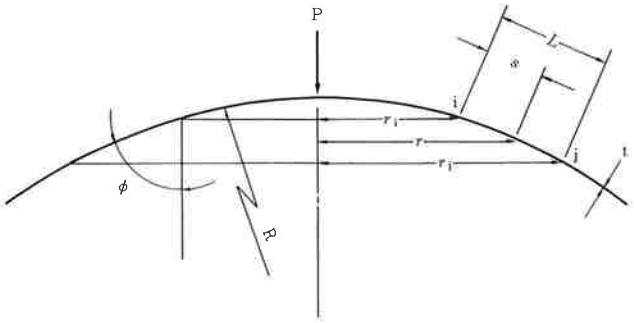

Fig. 5—Analysis of dome-spring.

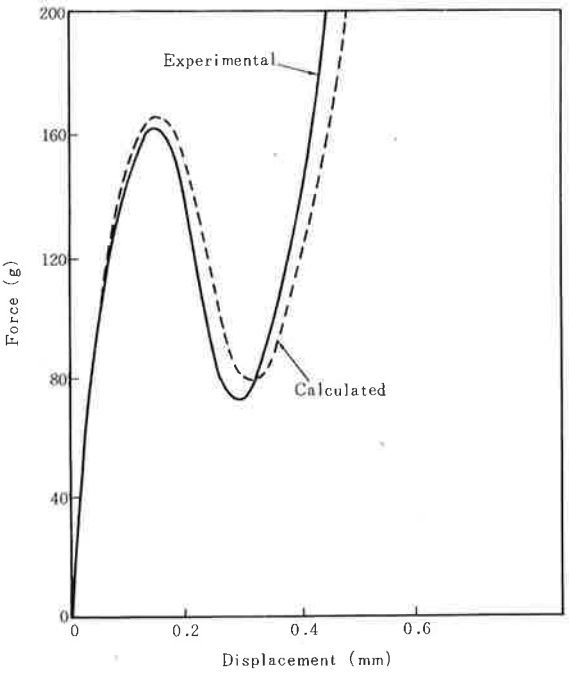

Fig. 6—Force-displacement characteristics of dome-spring.

where,

[D] : the stress-strain matrix

[B] : the strain-displacement matrix

and for an isotropic shell

$$[D] = \frac{Et}{1-\gamma^2}\begin{bmatrix} 1 & \gamma & 0 & 0 \\ \gamma & 1 & 0 & 0 \\ 0 & 0 & t^2/12 & \gamma t^2/12 \\ 0 & 0 & \gamma t^2/12 & t^2/12 \end{bmatrix} . \qquad \cdots\cdots\cdots\cdots (3)$$

Using equation (3), equation (2) may be written as follows.

$$[K] = \int_0^1 [B]^T [D][B]\, 2\pi r L ds' , \qquad \cdots\cdots\cdots\cdots\cdots (4)$$

where,

$s' \stackrel{\text{def}}{=} s/L$

and

$$[B] = \left[[B_i]\ [\lambda], [B_j]\ [\lambda]\right] . \qquad \cdots\cdots\cdots\cdots\cdots (5)$$

Provided that

$$[B_i] = \left[\begin{array}{c|c|c} -1/L & 0 & 0 \\ (1-s')\sin\phi/r & (1-3s'^2+2s'^3)\cos\phi/r & L(s'-2s'^2+s'^3)\cos\phi/r \\ 0 & (-6+12s')/L^2 & (-4+6s')/L \\ 0 & (6s'-6s'^2)\sin\phi/rL & (-1+4s'-3s'^2)\sin\phi/r \end{array}\right]$$

$$[B_j] = \left[\begin{array}{c|c|c} 1/L & 0 & 0 \\ s'\sin\phi/r & (3s'^2-2s'^3)\cos\phi/r & L(-s'^2+s'^3)\cos\phi/r \\ 0 & (6-12s')/L^2 & (-2+6s')/L \\ 0 & (-6s'+6s'^2)\sin\phi/rL & (2s'-3s'^2)\sin\phi/r \end{array}\right]$$

$$[\lambda] = \begin{bmatrix} \cos\phi & \sin\phi & 0 \\ -\sin\phi & \cos\phi & 0 \\ 0 & 0 & 1 \end{bmatrix}$$

$r = (1-s')\, r_i + s' r_j$.

Equation (4) was integrated using Gause-Legendre quadrature. The nonlinear force displacement characteristic of the dome-spring was analyzed by computer according to the incremental load procedure. After prototype test production, it was found that the actual characteristic values of the dome-spring coincided almost perfectly with the calculated values, as shown in Fig. 6.

2.2 Design of actuator

The main points of the actuator design were as follows:

1) How to fasten it as a cantilever.
2) Where to place the projection for pushing the dome-spring.
3) How to avoid concentration of stress around the projection.

Consideration of these points led to the shape shown in Fig. 7.

The touch characteristic of the actuator was analyzed as a contilever beam of discontinuous cross-section, as shown in Fig. 8.

The beam was divided into j subelements. The depressing force P and displacement W at the depressing point j can be expressed as a function of the reaction force R and displacement δ of the dome-spring at the point i.

$$P = \frac{\delta + R\left[\sum_{m=1}^{i} g_m^R + \sum_{m=1}^{i}\left\{(l_m - l_{m-1})\sum_{k=1}^{m-1} f_k^R\right\}\right]}{\sum_{m=1}^{i} g_m^P + \sum_{m=1}^{i}\left\{(l_m - l_{m-1})\sum_{k=1}^{m-1} f_k^P\right\}} \quad \cdots\cdots (6)$$

$$W = P\left[\sum_{m=1}^{j} g_m^P + \sum_{m=1}^{j}\left\{(l_m - l_{m-1})\sum_{k=1}^{m-1} f_k^P\right\}\right] - R\left[\sum_{m=1}^{i} g_m^R + \sum_{m=1}^{i}\left\{(l_m - l_{m-1})\sum_{k=1}^{m-1} f_k^R\right\}\right] + (l_j - l_i)\sum_{m=1}^{i} f_m^R\Big], \quad \cdots\cdots\cdots\cdots\cdots\cdots (7)$$

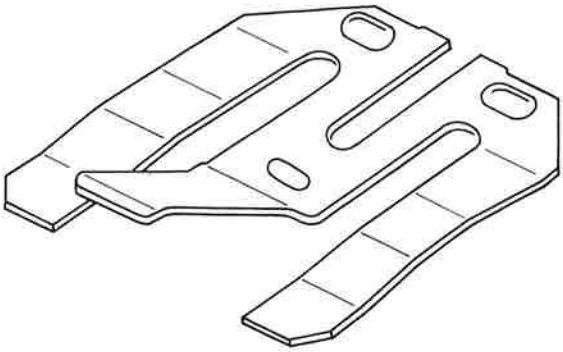

Fig. 7—Actuator shape.

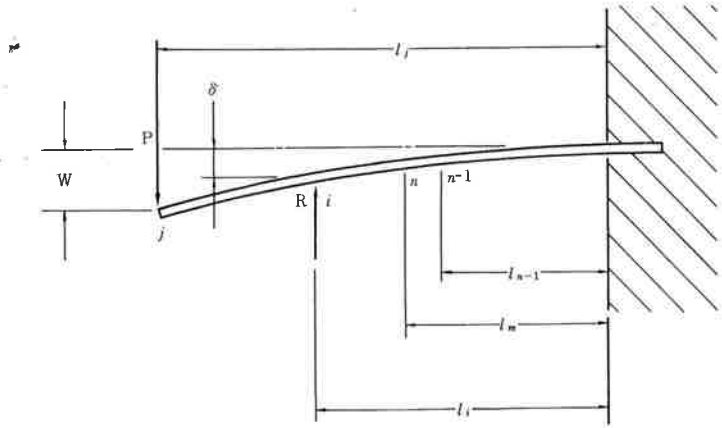

Fig. 8—Cantilever beam of discontinuous cross-section.

where,

$$f_n^P = (1/EI_n)\ \{(l_j - l_{n-1})(l_n - l_{n-1}) - (l_n - l_{n-1})^2/2\}$$

$$f_n^R = (1/EI_n)\ \{(l_i - l_{n-1})(l_n - l_{n-1}) - (l_n - l_{n-1})^2/2\}$$

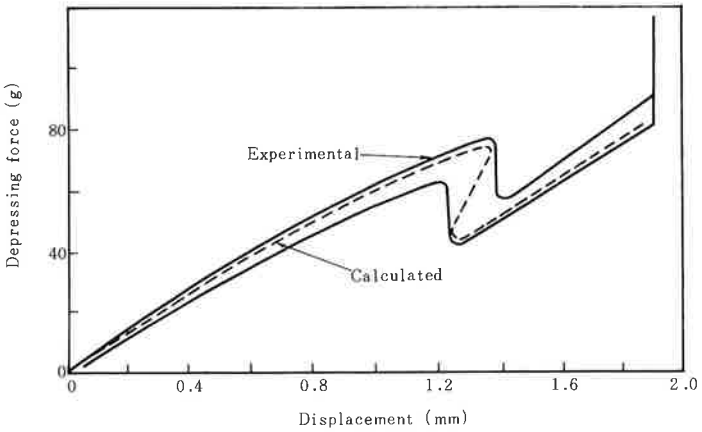

Fig. 9–Comparison between calculated and experimental values.

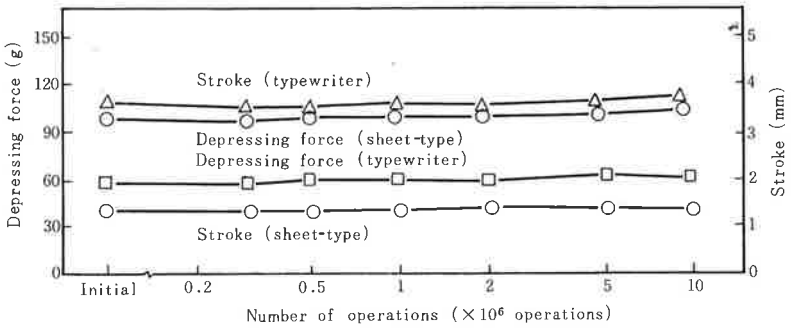

Fig. 10–Life characteristics.

$$g_n^P = (1/6EI_n)\ \{3(l_j - l_{n-1})(l_n - l_{n-1})^2 - (l_n - l_{n-1})^3\}$$

$$g_n^R = (1/6EI_n)\ \{3(l_i - l_{n-1})(l_n - l_{n-1})^2 - (l_n - l_{n-1})^3\}\ . \quad \cdots\cdots\ (8)$$

δ : Deflection of dome-spring

R : Reaction force of dome-spring
E : Modulus of elasticity
l_n : Length between bases and n-th node
I_n : Moment of inertia of area
$I_n = b_n h^3/12$, b_n : Width of n-th element
h : Thickness of actuator.

Equations (6) and (7) were evaluated by computer, using the characteristics of the dome-spring.

Trial production based on these calculations showed that the calculated values coincided closely with the experimental values (see Fig. 9). In addition, the operational characteristics of the lifetime of the switch turned out to be extremely stable (see Fig. 10).

3. Reliability

Most terminals provide a keyboard, display, controller, and power source. The controller and power source have been simplified by use of microprocessors and their reliability has been improved. Therefore the reliability of the device tends to be governed by that of the keyboard or display. Keyboard reliability is most greatly influenced by the reliability of the switches.

The contact in the switch was designed as shown in Fig. 11.

In this design, the depressing force is added to the tension of dome-spring through the actuator and keytop, so that even if the keyboard is operated with various forces, a constant force is always transferred to the contact.

The energy of the key operation is transmitted to the contact so that the contact force is always more than 40 g.

Spherical multicontacts were adopted to give a steady contact reliability. On the basis of the experiments shown in Figs. 12 and 13, they were partially plated with gold, 1 μm in thickness.

The contacts were also covered with a plastic seal to protect them from dust and corrosive gas.

Actually contact resistance and bounce time were extremely stable during the lifetime test shown in Fig. 14.

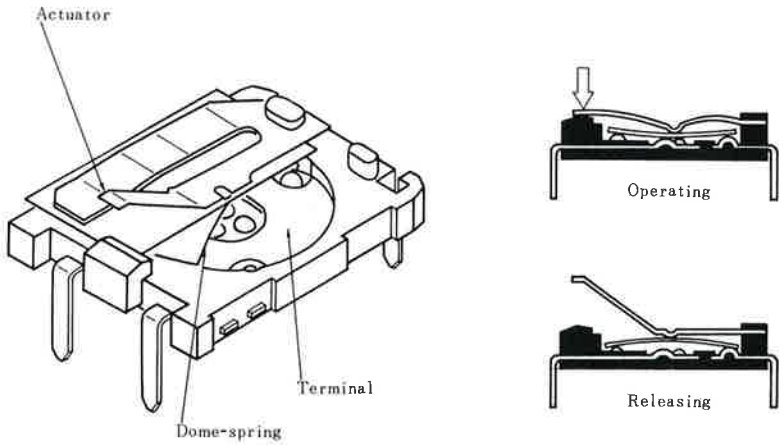

Fig. 11—Construction of mechanical switch.

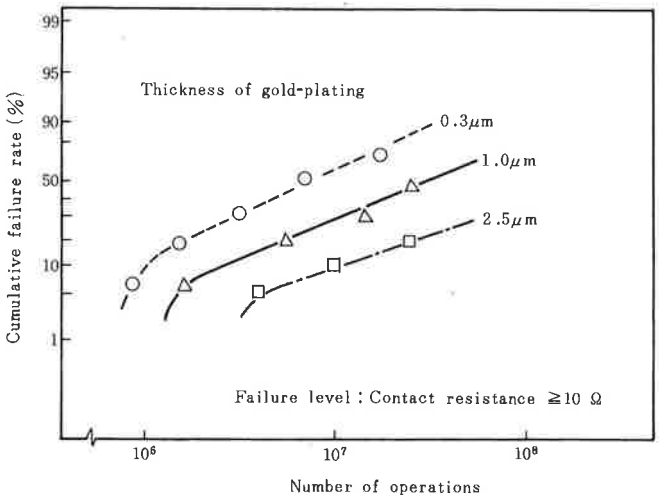

Fig. 12—Investigation of gold-plating.

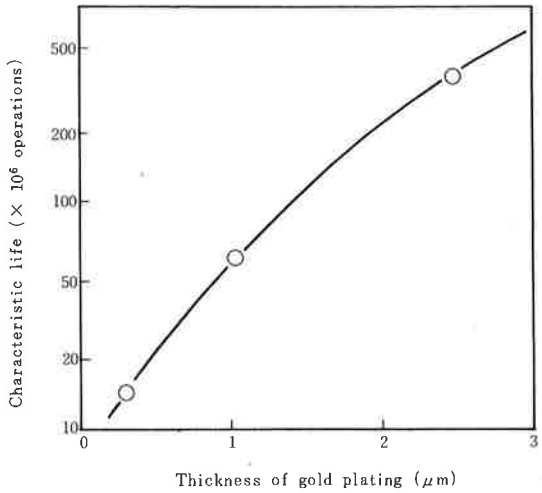

Fig. 13—Investigation of gold-plating.

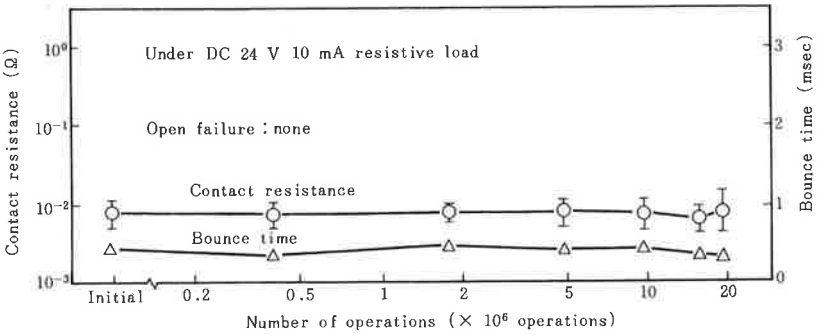

Fig. 14—Lifetime characteristics.

4. Economy

In order to realize economical production, a hoop shaped, molded lot of continuously connected components is processed, assembled, and tested in the fully-automatic process shown in Fig. 15.

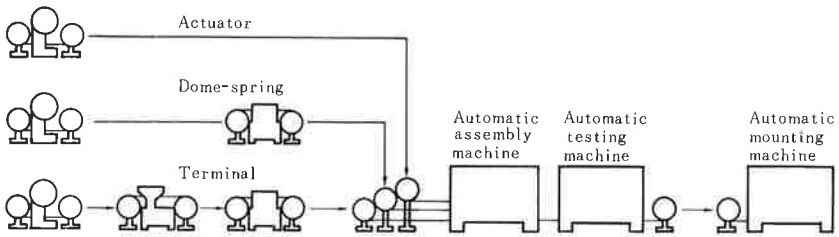

Fig. 15–Mechanical switch assembly line.

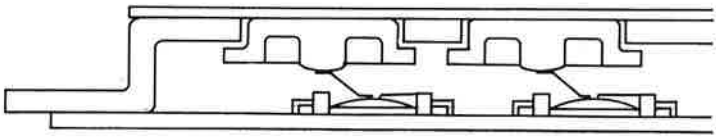

Fig. 16–Construction of sheet-type keyboard.

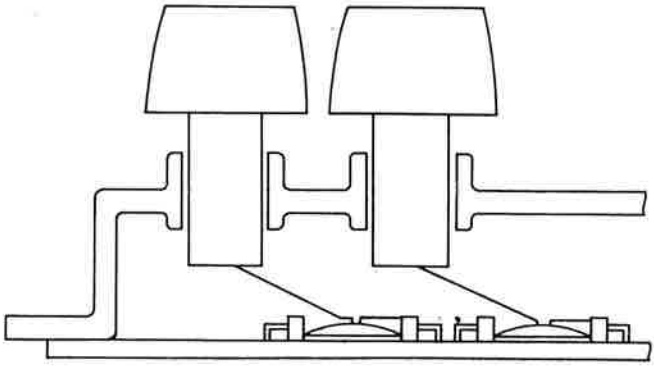

Fig. 17–Construction of typewriter keyboard.

The newly designed switch has made it possible to produce models for both sheet-type and typewriter keyboards (see Figs. 16 and 17) by changing only the length of the actuator, and to unify the housing and panel, thus simplifying over-

Fig. 18—Appearance of sheet-type keyboard.

Fig. 19—Appearance of typewriter keyboard.

all keyboard construction.

In addition, the standardized construction makes it possible to design many kinds of keyboards with the aid of the computer.

This CAD (Computer Aided Design) permits the customer to create the exact keyboard desired to meet his individual needs and preferences.

By means of CAD, and by supplying PCB (Printed Circuit Board) work films

Table 1. Characteristics of keyboard

Mechanical Characteristics	
Depressing force	Sheet-type: 100 g Typewriter: 60 g
Stroke	Sheet-type: 1.3 mm Typewriter: 3.5 mm
Electrical Characteristics	
Contact rating	DC 24 V 50 mA
Contact resistance	1 Ω max DC 6 V 10 mA
Insulation resistance	50 MΩ min DC 250 V
Dielectric withstanding voltage	DC 250 V min
Bounce time	5 msec max
Environmental Characteristics	
Operating temperature	0 °C to +50 °C
Storage temperature	−20 °C to +50 °C
Humidity	+40 °C 90-95 %RH 48 h
Vibration	10 to 55 Hz 1.5 mm
Shock	10 G 11 msec
Lifetime	More than 5×10^6 operations DC 24 V 10 mA Resistive load

and numerical control tapes for the panel stamping press to the production process, and by mounting the switches on the PCB automatically, total cost reduction has been achieved.

The appearance of keyboards using the new switches is shown in Figs. 18 and 19. Characteristics of these keyboards are shown in Table 1.

5. Conclusion

The results of this project can be summerized as follows:

1) A mechanical switch has been developed which has optimum operational characteristics, achieved by combining an actuator and a dome-spring, and high reliability, achieved through use of gold-plated multi-contacts.

2) This switch is economical and can be applied to both sheet-type and typewriter keyboards by changing only the length of the actuator.
3) Using these designed switches, the sheet-type keyboard covered with a sheet that can be printed with a multi-color design has been developed.
4) Using these designed switches, the typewriter keyboard which combines economical construction with excellent operational characteristics has been developed.

6. Acknowledgement

The authors wish to express their deep appreciation to Dr. H. Sasaki for his splendid guidance and also to Messrs. T. Tanaka and T. Sasaki for their co-operation.

References

1) R. Kinoshita et al: "Reliability and Applications of Magnet Driven Reed Switch," Proc. 20th Relay Conf., (1972).
2) O. C. Zienkiewicz and Y. K. Cheung: The finite element method in structural and continuum mechanics, McGraw-Hill, Berkshire, (1967).